

Portland State University

PDXScholar

Center for Electron Microscopy and
Nanofabrication Publications and Presentations

Center for Electron Microscopy and
Nanofabrication

2008

Nano Quasicrystal Formation and Local Atomic Structure in Zr–Pd and Zr–Pt Binary Metallic Glasses

Junji Saida

Center for Interdisciplinary Research

Takashi Sanada

Research Department, Nissan ARC Ltd

Shigeo Sato

Institute for Materials Research

Muneyuki Imafuku

Materials Characterization Center, Nippon Steel Technoresearch Corp.

Chunfei Li

Center for Electron Microscopy and Nanofabrication

Follow this and additional works at: https://pdxscholar.library.pdx.edu/cemn_pub

 [Part of the Center for Electron Microscopy and Nanofabrication Commons](#), and the [Semiconductor and Optical Materials Commons](#)

Let us know how access to this document benefits you.

Citation Details

Saida, J., Sanada, T., Sato, S., Imafuku, M., Li, C., & Inoue, A. (2008). Nano quasicrystal formation and local atomic structure in Zr–Pd and Zr–Pt binary metallic glasses. *Zeitschrift für Kristallographie*, 223(11-12), 726-730.

This Article is brought to you for free and open access. It has been accepted for inclusion in Center for Electron Microscopy and Nanofabrication Publications and Presentations by an authorized administrator of PDXScholar. Please contact us if we can make this document more accessible: pdxscholar@pdx.edu.

Authors

Junji Saida, Takashi Sanada, Shigeo Sato, Muneyuki Imafuku, Chunfei Li, and Akihisa Inoue

Nano quasicrystal formation and local atomic structure in Zr–Pd and Zr–Pt binary metallic glasses

Junji Saida^{*,I}, Takashi Sanada^{II}, Shigeo Sato^{III}, Muneyuki Imafuku^{IV}, Chunfei Li^V and Akihisa Inoue^{VI}

^I Center for Interdisciplinary Research, Tohoku University, Sendai 980-8578, Japan

^{II} Research Department, Nissan ARC Ltd., Yokosuka 237-0061, Japan

^{III} Institute for Materials Research, Tohoku University, Sendai 980-8577, Japan

^{IV} Materials Characterization Center, Nippon Steel Technoresearch Corp., Chiba, 293-0011, Japan

^V Center for Electron Microscopy and Nanofabrication, Portland State University, Portland, OR 97207, USA

^{VI} President, Tohoku University, Sendai 980-8577, Japan

Received June 6, 2008; accepted July 18, 2008

Metallic glass / Icosahedral quasicrystal / Local structure / Transformation / Zr-based alloy

Abstract. Formation of the nanoscale icosahedral quasicrystalline phase (I-phase) in the melt-spun Zr₇₀Pd₃₀ and Zr₈₀Pt₂₀ binary metallic glasses were reported. Local atomic structure in the glassy and quasicrystal (QC)-formed states were also analyzed by XRD and EXAFS measurements in order to investigate the formation mechanism of QC phase. The distorted icosahedral-like local structure can be identified around Zr atom in the Zr₇₀Pd₃₀ metallic glass. In the QC formation process, a change of local environment around Zr is detected, in which the approximately one Zr atom substitutes for one Pd atom. In contrast, since the local environment around Pt atom is remaining during the QC precipitation, it is suggested that the stable icosahedral local structure is mainly formed around a center Pt atom in the glassy state in Zr₈₀Pt₂₀. We also found that the local environment around Zr atom significantly changes during the quasicrystallization in the alloy. These results differ from those in the Zr₇₀Pd₃₀ metallic glass.

Introduction

A number of studies on nanoquasicrystallization in Zr–Al–Ni–Cu multicomponent metallic glasses by the additional elements [1–4] or oxygen impurity [5, 6] have led us to new aspects of the local structure investigation in the glassy state. It has been reported that the Zr-based metallic glasses with high glass-forming ability (GFA) have unique local structure in the glassy state [7]. The nano icosahedral quasicrystalline phase (I-phase) formation exhibits the possibility of a common structure between the I-phase and local atomic configuration in the glassy state [8]. Actually, we have reported the local structural similarity between the glassy and quasicrystal (QC)-formed states

in the Zr–Al–Ni metallic glass [9]. Based on the series of local structural studies, the authors have obtained a conclusion that the stability of supercooled liquid state, *i.e.* GFA is strongly correlated with the formation of icosahedral local structure in Zr-based alloys [8, 10–12].

It has been also reported the I-phase formation in the binary Zr–Pd and Zr–Pt metallic glasses [13–16]. The results may indicate that the icosahedral local structure is formed in the corresponding binary systems as well as multicomponent metallic glasses with a stable supercooled liquid state. Takagi *et al.*, have investigated that a considerable number of icosahedral clusters are presented around Zr atom in the as-quenched state and the number of them increases by QC precipitation in the Zr₇₀Pd₃₀ binary metallic glass using the electron diffraction structure analysis [17]. They have speculated the easy precipitation of nano I-phase by the quenched-in icosahedral clusters around Zr atom. In this paper, we investigate the detailed structure analysis and local environment around constitutional elements in the nano QC-forming Zr₇₀Pd₃₀ and Zr₈₀Pt₂₀ metallic glasses by radial distribution function (RDF) analysis using X-ray diffraction and X-ray absorption fine structure (EXAFS) studies. From these studies, we intend to report the structural characterization of the two glassy alloys with a comparison of the local environment in the glassy and QC-formed states.

Experimental procedure

The master ingots of the Zr₇₀Pd₃₀ and Zr₈₀Pt₂₀ alloys were produced by arc-melting high purity metals of 99.9 mass% Zr, 99.9 mass% Pd and 99.98 mass% Pt in a purified argon atmosphere. The glassy ribbon was prepared by single roller melt quenching technique. The oxygen content of the both ribbons was in the level less than 700 mass ppm. The sample was annealed in a vacuum atmosphere. The thermal stability of the as-quenched sample was analyzed by differential scanning calorimetry (DSC) at a heating rate of 0.67 K/s. The annealed structure was examined by

* Correspondence author (e-mail: jsaida@cir.tohoku.ac.jp)

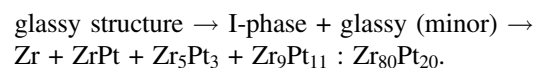
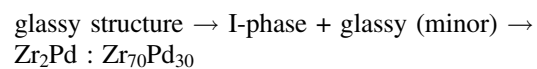
transmission electron microscopy (TEM) with an accelerating voltage of 200 kV in addition to the X-ray diffractometry (XRD) analysis with $\text{CuK}\alpha$ radiation at 40 kV–40 mA. The sample for TEM observation was prepared by the ion milling technique. The local atomic structure was studied by ordinary X-ray diffraction measurements with monochromatic $\text{MoK}\alpha$ radiation of 50 kV–200 mA produced by a rotating anode X-ray generator. The scattered X-ray intensities were corrected for air-scattering, absorption, polarization effects and converted to electron units per atom by the generalized Krogh–Moe–Norman method to obtain an interference function, $Q_i(Q)$ estimated from the coherent scattering intensity in absolute units. The ordinary RDF was led by Fourier transformation of the $Q_i(Q)$. The coordination number, N and interatomic distance, r between the constituent elements were calculated by fitting the $Q_i(Q)$ and RDF with non-linear least square fitting method. EXAFS measurements for the analysis of local environment around Zr, Pd and Pt atoms were performed at SPring-8 synchrotron radiation on beam line BL01B1. All measurements were done in transmission geometry at room temperature. Measured spectra were analyzed using the program REX 2000 (Rigaku Corp.). The EXAFS simulation of each structure model was performed using the FEFF 8.2 code [18].

Results and discussion

Nano quasicrystallization process

No significant X-ray diffraction peaks except a halo peak are observed and homogeneous high-resolution TEM images without an obvious fringe contrast originated from the (quasi)crystalline phase are also obtained in the as-quenched $\text{Zr}_{70}\text{Pd}_{30}$ and $\text{Zr}_{80}\text{Pt}_{20}$ alloys [19]. DSC curves of the melt-spun $\text{Zr}_{70}\text{Pd}_{30}$ and $\text{Zr}_{80}\text{Pt}_{20}$ metallic glasses and XRD patterns of the annealed samples are shown in Fig. 1(a) and (b), respectively. In the $\text{Zr}_{70}\text{Pd}_{30}$ metallic glass, the crystallization proceeds through two exothermic reactions and the crystallization temperature T_x corresponding to the onset temperature of the first exothermic peak is 723 K. The temperature interval between the two exothermic peaks is approximately 80 K. Although the two-stage crystallization process is also observed in the $\text{Zr}_{80}\text{Pt}_{20}$ metallic glass, the exothermic peaks are weaker and broader than those in the $\text{Zr}_{70}\text{Pd}_{30}$ alloy. The onset

temperature of the first exothermic peak is 717 K and peak temperatures of the two exothermic reactions are 757 and 923 K, respectively. For the determination of the primary phase transformed from the glassy state, we examined structure of the samples annealed for 900 s at 620 K for the $\text{Zr}_{70}\text{Pd}_{30}$ alloy and for 300 s at 820 K for the $\text{Zr}_{80}\text{Pt}_{20}$ alloy as shown in Fig. 1(b). All the diffraction peaks can be identified as an icosahedral phase. High-resolution TEM images of the annealed $\text{Zr}_{70}\text{Pd}_{30}$ and $\text{Zr}_{80}\text{Pt}_{20}$ alloys are shown in Fig. 2(a) and (b), respectively. Fine particles with diameters less than 20 nm are homogeneously distributed in the glassy matrix in both alloys. A typical fast Fourier transformation (FFT) pattern from the precipitated particles shown in Fig. 2(c) clearly indicates the fivefold symmetry, which reveals that the first exothermic peak corresponds to the transformation from glassy to icosahedral phase. We have already reported the transformation processes of the $\text{Zr}_{70}\text{Pd}_{30}$ and $\text{Zr}_{80}\text{Pt}_{20}$ metallic glasses in the isochronal annealing of the heating rate of around 0.67 K/s as follows [19];



Local structure evaluation in $\text{Zr}_{70}\text{Pd}_{30}$ and $\text{Zr}_{80}\text{Pt}_{20}$ metallic glasses

The radial distribution function (RDF) curves of the as-quenched $\text{Zr}_{70}\text{Pd}_{30}$ and $\text{Zr}_{80}\text{Pt}_{20}$ metallic glasses obtained from the Fourier transformation of interference function, $Q_i(Q)$ are shown in Figs. 3 (a) and (b), respectively. The fit positions of the Zr–Zr, Zr–Pd, Pd–Pd, Zr–Pt and Pt–Pt pairs are indicated in the RDF curves. Based on the RDF curves, calculation of nearest neighbor atomic distances, r and coordination numbers, N is summarized in Table 1. The fitting results in the QC-formed state are also denoted in the table. We have also considered some of the fitting results of each atom by the anomalous X-ray scattering analysis (AXS) to justify the distance of atomic pair and coordination number in the table [20, 21]. We can suggest the icosahedral-like local structure in the $\text{Zr}_{70}\text{Pd}_{30}$ metallic glass because of the total coordination number of 12.0 around Zr atom. On the other hand, it is 9.2 around Pd atom, which implies that the icosahedral local structure is formed around Zr rather than Pd atoms. The results

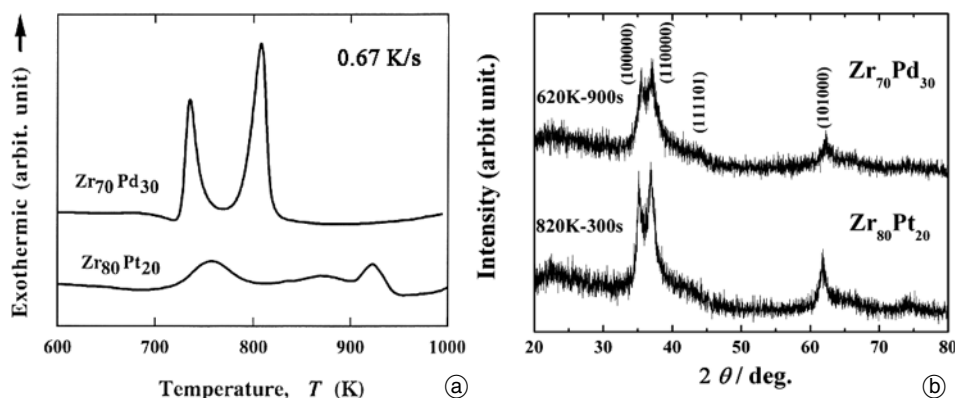


Fig. 1. DSC curves (a) of the melt-spun $\text{Zr}_{70}\text{Pd}_{30}$ and $\text{Zr}_{80}\text{Pt}_{20}$ metallic glasses and XRD patterns (b) of the samples annealed for 900 s at 620 K for the $\text{Zr}_{70}\text{Pd}_{30}$ alloy and for the 300 s at 820 K for the $\text{Zr}_{80}\text{Pt}_{20}$ alloy.

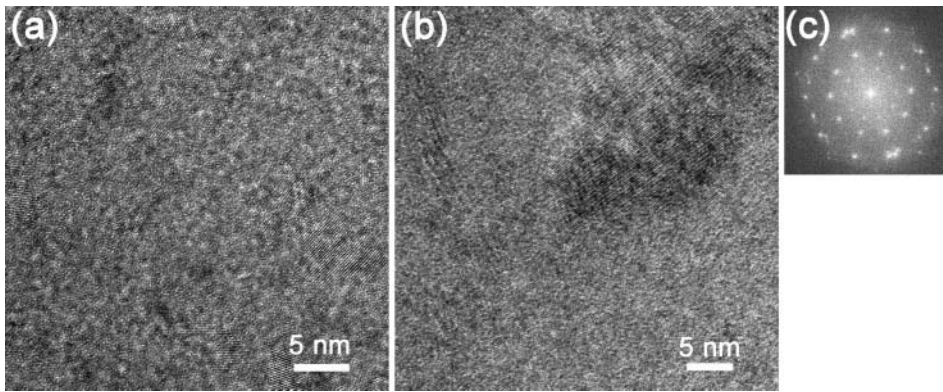


Fig. 2. High-resolution TEM (HREM) images of the $Zr_{70}Pd_{30}$ alloy (a) annealed for 900 s at 620 K and $Zr_{80}Pt_{20}$ alloy (b) annealed for 300 s at 820 K. Typical FFT pattern taken from the precipitated particles in HREM image is also shown in (c).

agree with those analyzed by electron diffraction and the Voronoi-polyhedra analysis, in which the icosahedral-like and prism-like clusters are formed around Zr and Pd atoms, respectively [17]. The icosahedral-like local structure should be slightly distorted considering that the distance of Zr–Pd pair (approximately 0.289 nm) is shorter than the sum of the atomic radii of Zr (0.162 nm) and Pd (0.137 nm). Moreover, we can point out a change of local environment around Zr in the QC formation process even in the formation of icosahedral-like local structure around Zr atom in the glassy state. Comparing the coordination numbers of Zr–Zr and Zr–Pd between the glassy and QC-formed states, it is found the approximately one Zr atom substitutes for one Pd atom during QC precipitation. Meanwhile, the change in local environment around Pd is considerably less than that of Zr. We investigate that this kind of rearrangement may improve the structural perfection of the quenched-in icosahedral-like local structure, leading to the phase evolution of I-phase [22]. This suggestion is also supported by the compositional difference between the residual glassy region and I-phase analyzed by EDX measurements [19].

The pair distance of Zr–Zr can be fitted by 0.326 nm, which is not so different from the calculated value of 0.320 nm in the $Zr_{80}Pt_{20}$ metallic glass. In contrast, the distance of the Pt–Pt pair (0.326 nm) is significantly longer than the expected value (approximately 0.278 nm) from its atomic radius, which implies that the Pt atom forms a new local structure with Zr atom by the strong chemical affinity. The total coordination numbers around Zr and Pt are 11.1 and 12.1, respectively. Since the total coordination number around Pt is close to 12.0, we point out a possibility of existence of an icosahedral-like local environment in the center of Pt atom. In the QC-formed state, the total coordination numbers around Zr and Pt atoms are 14.2 and 12.4, respectively. Especially, the later coordination number also supports the suggestion of the icosahedral-like environment around Pt atom [20]. The distance of all pairs is almost the same in the both states, however, it is found that the rearrangement occurs especially around

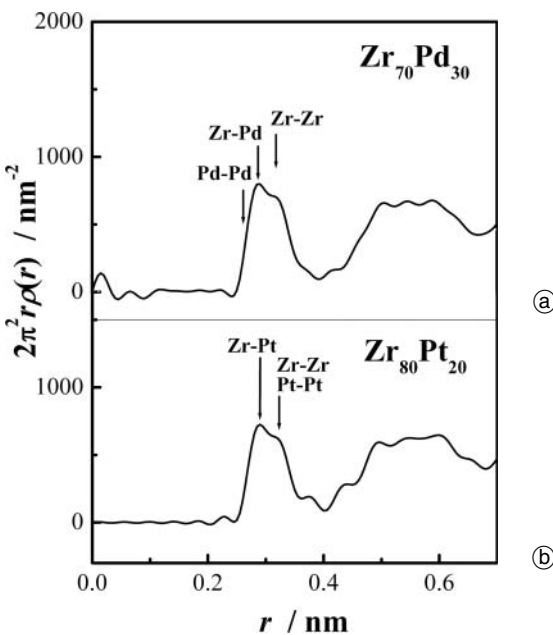


Fig. 3. Radial distribution function (RDF) curves of the $Zr_{70}Pd_{30}$ (a) and $Zr_{80}Pt_{20}$ (b) metallic glasses (RDF) obtained from the Fourier transformation of $Q_i(Q)$.

Table 1. Calculated nearest neighbor atomic distances (r) and coordination numbers (N) from RDF results in the as-quenched $Zr_{70}Pd_{30}$ and $Zr_{80}Pt_{20}$ metallic glasses. The fitting results in the QC-formed state are also denoted in the table.

		Pairs	r (nm)	N
$Zr_{70}Pd_{30}$	as-quenched	Zr–Zr	0.326 ± 0.002	8.3 ± 0.4
		Zr–Pd	0.289 ± 0.001	3.7 ± 0.2
		(Pd–Zr)		(8.6 ± 0.2)
		Pd–Pd	0.273 ± 0.002	0.6 ± 0.2
	QC-formed	Zr–Zr	0.320 ± 0.002	9.8 ± 0.6
		Zr–Pd	0.281 ± 0.002	2.5 ± 0.2
		(Pd–Zr)		(5.8 ± 0.2)
		Pd–Pd	0.265 ± 0.002	0.3 ± 0.2
$Zr_{80}Pt_{20}$	as-quenched	Zr–Zr	0.326 ± 0.002	8.8 ± 0.3
		Zr–Pt	0.286 ± 0.001	2.3 ± 0.2
		(Pt–Zr)		(9.3 ± 0.2)
		Pt–Pt	0.326 ± 0.002	1.8 ± 0.2
	QC-formed	Zr–Zr	0.323 ± 0.001	11.8 ± 0.5
		Zr–Pt	0.291 ± 0.001	2.4 ± 0.2
		(Pt–Zr)		(9.5 ± 0.5)
		Pt–Pt	0.328 ± 0.001	2.9 ± 0.3

Zr atom due to the considerable change in the coordination number of Zr–Zr in the QC precipitation.

In order to examine the local structure around Zr, Pd and Pt atoms, we performed EXAFS measurements for the glassy and QC-formed states of $Zr_{70}Pd_{30}$ and $Zr_{80}Pt_{20}$ alloys. The Fourier transformation curves of EXAFS measurements of the Zr *K*-edge (a) and Pd *K*-edge (b) in the $Zr_{70}Pd_{30}$ alloy and Zr *K*-edge (c) and Pt *K*-edge (d) in the $Zr_{80}Pt_{20}$ alloy in the glassy and QC-formed states are shown in Fig. 4. The calculated results of the icosahedral cluster model, Zr_2Pd and Zr_5Pt_3 structures, which are the major precipitated phases after the decomposition of icosahedral phase in both alloys, are also shown in the figure. Especially, it is speculated that the Zr_5Pt_3 structure may have a relation of local structure in glassy state in Zr_xPt_{100-x} ($x = 73–77$) alloys [23]. The corresponding atomic structures of Zr_2Pd and Zr_5Pt_3 are also schemati-

cally denoted in Fig. 4 (e). Although no significant change in EXAFS spectra is observed around Pd atom between both states, the local environment around Zr in the QC-formed state slightly differs from that in the as-quenched state in the $Zr_{70}Pd_{30}$ alloy. The calculated EXAFS spectrum of the icosahedral cluster model in Zr *K*-edge is well fitted by that in the QC-formed state rather than the as-quenched one. These are consistency with the RDF results shown in Table 1. The reason for the local environment change in Zr *K*-edge during the QC precipitation, even if the icosahedral local structure is formed around Zr atom, may be its considerable distortion in the glassy state. It is also noted that all the experimental results around Zr and Pd atoms can not be fitted with the corresponding Zr_2Pd simulation results, indicating that the significant rearrangement of constitutional elements is necessary to precipitate the stable Zr_2Pd crystalline phase in the glassy and QC-formed states.

The atomic distribution changes during the precipitation of QC phase around Zr *K*-edge in the Fourier transformation curves as shown in Fig. 4(c) in the $Zr_{80}Pt_{20}$ alloy, exhibiting a necessity of the rearrangement of Zr atom for quasicrystallization. While the QC-formed state as well as the glassy state has a significantly different local environment from that of the Zr_5Pt_3 structure, the sharp peak around $r = 0.32$ nm in the measured one is similar to that of the icosahedral cluster model. However, the shoulder peak in the lower distance can not be fitted with the icosahedral cluster model. We have recently reported that the measured curve in Zr *K*-edge in the as-quenched state can be well fitted with the mixed local environment model, consisting of 60% icosahedral cluster and 40% Zr_5Pt_3 structure [24]. The well fitted curve changes into the model of 80% icosahedral cluster and 20% Zr_5Pt_3 structure in the QC-formed state. The increase of ratio of the icosahedral cluster in the fitted curve during the quasicrystallization is very reasonable. The 20% Zr_5Pt_3 local structure in the QC-formed state may be attributed to the residual glassy region after quasicrystallization.

In contrast, the Fourier transformation curves of the Pt *K*-edge in the as-quenched and QC-formed states resemble each other, indicating that the local environment does not change through the quasicrystallization. Moreover, they can be fitted by the icosahedral cluster model well rather than the Zr_5Pt_3 structure model. The obtained results exhibit the existence of the stable icosahedral local structure around Pt atom in the $Zr_{80}Pt_{20}$ metallic glass. These are also consistent to those of the RDF fitting. We point out that the tendency is significantly different from that in the QC-forming $Zr_{70}Pd_{30}$ metallic glass, in which the icosahedral local structure is formed around Zr atom [17]. Although it is still unclear for this reason in detail, we speculate that it may be due to several ones such as the difference of chemical affinity between Zr–Pd and Zr–Pt, and the structural correlation between the glassy and stable crystalline phases. In the present study, we can conclude that the formation of the stable icosahedral-like local structure in the glassy state strongly contributes to the QC-precipitation in the present binary alloys.

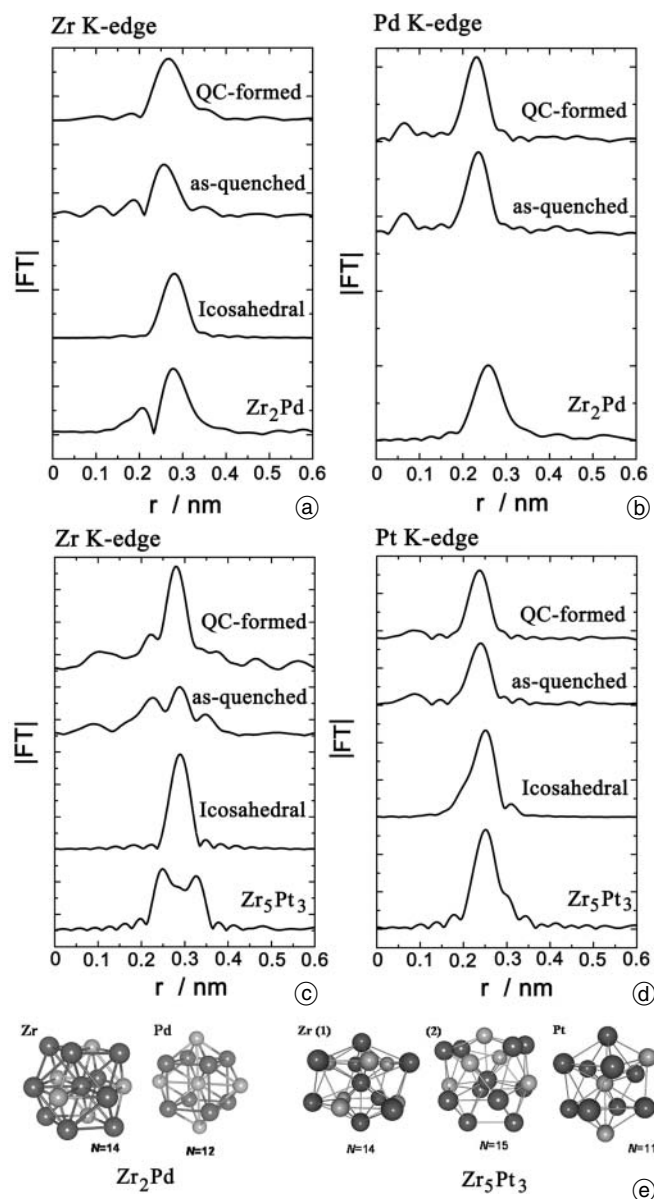


Fig. 4. Fourier transformation curves of EXAFS measurements of the Zr *K*-edge (a) and Pd *K*-edge (b) in the $Zr_{70}Pd_{30}$ alloy and Zr *K*-edge (c) and Pt *K*-edge (d) in the $Zr_{80}Pt_{20}$ alloy in the glassy and QC-formed states. The corresponding atomic structures of Zr_2Pd and Zr_5Pt_3 are schematically denoted in (e).

Conclusion

The present study provides the results of formation of the nano icosahedral quasicrystalline phase and local structural investigation of the $Zr_{70}Pd_{30}$ and $Zr_{80}Pt_{20}$ binary glassy alloys. We suggest an existence of the icosahedral local structure in the glassy state around Zr atom in the $Zr_{70}Pd_{30}$ alloy and Pt atom in the $Zr_{80}Pt_{20}$ alloy. In the QC formation process, a change of local environment around Zr is detected, in which the approximately one Zr atom substitutes for one Pd atom in the $Zr_{70}Pd_{30}$ alloy. In contrast, it is found the almost unchanged local environment around Pt atom and the significant change in local environment around Zr atom during the QC precipitation in the $Zr_{80}Pt_{20}$ alloy. These results differ from those in the $Zr_{70}Pd_{30}$ metallic glass.

Acknowledgments. This work is supported by Grant-in-Aid of the Ministry of Education, Sports, Culture, Science and Technology, Japan, Scientific Research (B), Priority Area on "Materials Science of Bulk Metallic Glasses" and "Science and Technology of Microwave-Induced, Thermally Non-Equilibrium Reaction Fields". It is also supported by Japan Science Promotion Society (JSPS), "Asian Core Program".

References

- [1] Chen, M. W.; Zhang, T.; Inoue, A.; Sakai, A.; Sakurai, T.: Quasicrystals in a partially devitrified $Zr_{65}Al_{7.5}Ni_{10}Cu_{12.5}Ag_5$ bulk metallic glass. *Appl. Phys. Lett.* **75** (1999) 1697–1699.
- [2] Inoue, A.; Zhang, T.; Saida, J.; Matsushita, M.; Chen, M. W.; Sakurai, T.: Formation of icosahedral quasicrystalline phase in Zr–Al–Ni–Cu–M (M = Ag, Pd, Au or Pt) systems. *Mater. Trans. JIM* **40** (1999) 1181–1184.
- [3] Saida, J.; Inoue, A.: Icosahedral quasicrystalline phase formation in Zr–Al–Ni–Cu glassy alloys by addition of Nb, Ta and V elements. *J. Phys. Condens. Matter* **13** (2001) L73–L78.
- [4] Xing, L. Q.; Eckert, J.; Löser, W.; Schultz, L.: High-strength materials produced by precipitation of icosahedral quasicrystals in bulk Zr–Ti–Cu–Ni–Al amorphous alloys. *Appl. Phys. Lett.* **74** (1999) 664–666.
- [5] Eckert, J.; Mattern, N.; Zinkevitch, M.; Seidel, M.: Crystallization behavior and phase formation in Zr–Al–Cu–Ni metallic glass containing oxygen. *Mater. Trans. JIM* **39** (1998) 623–632.
- [6] Murty, B. S.; Ping, D. H.; Hono, K.; Inoue, A.: Direct evidence for oxygen stabilization of icosahedral phase during crystallization of $Zr_{65}Cu_{27.5}Al_{7.5}$ metallic glass. *Appl. Phys. Lett.* **76** (2000) 55–57.
- [7] Matsubara, E.; Tamura, T.; Waseda, Y.; Inoue, A.; Zhang, T.; Masumoto, T.: Structural study of $Zr_{60}Al_{15}Ni_{25}$ amorphous alloys with a wide supercooled liquid region by the anomalous X-ray scattering (AXS) method. *Mater. Trans. JIM* **33** (1992) 873–878.
- [8] Saida, J.; Li, C.; Matsushita, M.; Inoue, A.: Investigation of the stability of glassy state in the Zr- and Hf-based glassy alloys correlated with their transformation behavior. *J. Mater. Res.* **16** (2001) 3389–3401.
- [9] Saida, J.; Imafuku, M.; Sato, S.; Sanada, T.; Matsubara, E.; Inoue, A.: Comparative study of local structure in $Zr_{70}Al_{10}Ni_{20}$ and quasicrystal-forming $Zr_{70}Al_9Ni_{20}Pd_1$ metallic glasses. *Phil. Mag. Lett.* **85** (2005) 135–144.
- [10] Saida, J.; Kasai, M.; Matsubara, E.; Inoue, A.: Stability of glassy state in Zr-based glassy alloys correlated with nano icosahedral phase formation. *Ann. Chim. Sci. Mater.* **27** (2002) 77–89.
- [11] Sato, S.; Sanada, T.; Saida, J.; Imafuku, M.; Matsubara, E.; Inoue, A.: Effect of Al on local structures in Zr–Ni and Zr–Cu metallic glasses. *Mater. Trans.* **46** (2005) 2893–2897.
- [12] Saida, J.; Imafuku, M.; Sato, S.; Sanada, T.; Matsubara, E.; Inoue, A.: Correlation between local structure and stability of supercooled liquid state in Zr-based metallic glasses. *Mater. Sci. Eng.* **A449–451** (2007) 90–94.
- [13] Murty, B. S.; Ping, D. H.; Hono, K.: Nanoquasicrystallization of binary Zr–Pd metallic glasses. *Appl. Phys. Lett.* **77** (2000) 1102–1104.
- [14] Saida, J.; Matsushita, M.; Li, C.; Inoue, A.: Formation of the icosahedral quasicrystalline phase in $Zr_{70}Pd_{30}$ binary glassy alloy. *Phil. Mag. Lett.* **81** (2001) 39–44.
- [15] Saida, J.; Matsushita, M.; Inoue, A.: Nanoscale icosahedral quasicrystalline phase formation in a rapidly solidified $Zr_{80}Pt_{20}$ binary alloy. *Appl. Phys. Lett.* **77** (2000) 73–75.
- [16] Sordelet, D. J.; Yang, X. Y.; Rozhkova, E. A.; Besser, M. F.; Kramer, M. J.: Oxygen-stabilized glass formation in $Zr_{80}Pt_{20}$ melt-spun ribbons. *Appl. Phys. Lett.* **83** (2003) 69–71.
- [17] Takagi, T.; Ohkubo, T.; Hirotsu, Y.; Murty, B. S.; Hono, K.; Shindo, D.: Local structure of amorphous $Zr_{70}Pd_{30}$ alloy studied by electron diffraction. *Appl. Phys. Lett.* **79** (2001) 485–487.
- [18] Ankudinov, A. L.; Ravel, B.; Rehr, J. J.; Conradson, S. D.: Real-space multiple-scattering calculation and interpretation of X-ray-absorption near-edge structure. *Phys. Rev. B* **58** (1998) 7565–7576.
- [19] Saida, J.; Matsushita, M.; Inoue, A.: Nano icosahedral quasicrystalline phase in Zr–Pd and Zr–Pt binary alloys. *J. Appl. Phys.* **90** (2001) 4717–4724.
- [20] Kitada, M.; Imafuku, M.; Saida, J.; Inoue, A.: Structural study of quasicrystallization in Zr–NM (NM = Pd or Pt) metallic glasses. *J. Non-Cryst. Solids* **312–314** (2002) 594–598.
- [21] Matsubara, E.; Nakamura, T.; Sakurai, M.; Imafuku, M.; Sato, S.; Saida, J.; Inoue, A.: Local atomic structures in amorphous and quasicrystalline $Zr_{70}Ni_{10}Pt_{20}$ and $Zr_{80}Pt_{20}$ alloys by the anomalous X-ray scattering method. *Mater. Res. Soc. Symp. Proc.* **644** (2001) L1.1.1–L1.1.12.
- [22] Imafuku, M.; Saida, J.; Inoue, A.: Change in local atomic structure during formation of icosahedral quasicrystalline phase in $Zr_{70}Pd_{30}$ glassy alloy. *J. Mater. Res.* **16** (2001) 3046–3049.
- [23] Sordelet, D. J.; Ott, R. T.; Li, M. Z.; Wang, S. Y.; Wang, C. Z.; Besser, M. F.; Liu, A. C. Y.; Kramer, M. J.: Structure of Zr_xPt_{100-x} ($73 = x = 77$) metallic glasses. *Met. Mater. Trans. A* **39A** (2008) 1908–1916.
- [24] Saida, J.; Sanada, T.; Sato, S.; Imafuku, M.; Inoue, A.: Local structure characterization in quasicrystal-forming $Zr_{80}Pt_{20}$ binary amorphous alloy. *Appl. Phys. Lett.* **91** (2007) 111901–1–3.